Author Manuscript

Author Manuscript

Author Manuscript

Author Manuscript

HHS Public Access

Author manuscript

Pediatr Res. Author manuscript; available in PMC 2019 December 27.

Published in final edited form as:

Pediatr Res. 2020 July ; 88(1): 66–76. doi:10.1038/s41390-019-0472-y.

A direct comparison of mouse and human intestinal development using epithelial gene expression patterns

Amy H. Stanford[1], **Huiyu Gong**[1], **Mackenzie Noonan**[1], **Angela N. Lewis**[2], **Qingqing Gong**[2], **Wyatt E. Lanik**[2], **Jonathan J. Hsieh**[3], **Shiloh R. Lueschow**[4], **Mark R. Frey**[3], **Misty Good**[2,*,#], **Steven J. McElroy**[1,4,#]

[1]Stead Family Department of Pediatrics, University of Iowa, Iowa City, IA

[2]Department of Pediatrics; Washington University School of Medicine; St Louis, MO

[3]Department of Pediatrics and of Biochemistry &Molecular Medicine; The Saban Institute at Children's Hospital Los Angeles, University of Southern California, Los Angeles, CA

[4]Department of Microbiology and Immunology, University of Iowa, Iowa City, IA

Abstract

PURPOSE: Preterm infants are susceptible to unique pathology due to their immaturity. Mouse models are commonly used to study immature intestinal disease including necrotizing enterocolitis (NEC). Current NEC models are performed at a variety of ages, but data directly comparing intestinal developmental stage equivalency between mice and humans are lacking.

METHODS: Small intestines were harvested from C57B1/6 mice at 3–4-day intervals from birth to P28 (n=8 at each age). Preterm human small intestine samples representing 17–23 weeks of completed gestation were obtained from the University of Pittsburgh Health Sciences Tissue Bank, and at term gestation during reanastamoses after resection for NEC (n=4–7 at each age). Quantification of intestinal epithelial cell types and mRNA for marker genes were evaluated on both species.

RESULTS: Overall, murine and human developmental trends over time are markedly similar. Murine intestine prior to P10 is most similar to human fetal intestine prior to viability. Murine

Users may view, print, copy, and download text and data-mine the content in such documents, for the purposes of academic research, subject always to the full Conditions of use:http://www.nature.com/authors/editorial_policies/license.html#terms

[*]**Corresponding Author:** Misty Good, MD, MS, Washington University School of Medicine, 660 S. Euclid Avenue, Campus Box 8208, St. Louis, MO 63110, mistygood@wustl.edu, 314-286-1329.

Contribution Statement: AHS, SRL, MRF, MG, SJM had full access to all the data in the study and take responsibility for the integrity of the data and the accuracy of the data analysis. Drs. Misty Good and Steven McElroy are co-senior/corresponding authors. All authors reviewed the results and approved the final version of the manuscript.

Concept and design: AHS, MRF, MG, SJM

Acquisition, analysis, and interpretation of data: AHS, HG, MN, ANL, QG, WEL, JJH, SRL, MRF, MG, SJM conducted all experimental bench work and contributed to sample analyses.
QG and MG maintained the clinical database.

*Statistical analysis:*AHS, ANL, QG, WEL, SRL, MG, SJM

*Manuscript preparation, drafting and critical revisions:*AHS, HG, MN, ANL, QG, WEL, JJH, SRL, MRF, MG, SJM prepared, drafted and critically revised the manuscript.

*Study supervision:*MRF, MG, SJM

[#]denotes equal contribution

Category of study: Basic Science

Disclosure Statement: The authors have no financial disclosures or conflicts of interest.

Author Manuscript Author Manuscript Author Manuscript Author Manuscript

intestine at P14 is most similar to human intestine at 22–23 weeks completed gestation, and P28 murine intestine is most similar to human term intestine.

CONCLUSION: Use of C57BL/6J mice to model the human immature intestine is reasonable, but the age of mouse chosen is a critical factor in model development.

Introduction

Global studies estimate that 15 million infants are born prematurely each year, and one million die as a direct result of their prematurity, making preterm birth the leading cause of mortality for children less than 5 years of age(l). Preterm infants are unique due to the immaturity of their organ systems, which leaves them highly susceptible to developing unique disease processes(2, 3). We seek to understand the role of intestinal immaturity during necrotizing enterocolitis (NEC) development, which remains one of the leading causes of death in premature infants(2, 3). Despite this significant morbidity and mortality, NEC is poorly understood and the precise etiology is still undefined. Because of this, animal models are required to study NEC and have played a critical role in our understanding of the disease to date(4), allowing for mechanistic studies of different biochemical pathways, specific cellular receptor signaling, and measurement of intestinal permeability which are technically difficult or impossible to study in humans(4).

Since the 1980s, several NEC mouse models have been proposed. Jilling used mice delivered via cesarean section at e20–21, which were exposed to hypoxia and formula feeding on postnatal day 0 (P0)(5). Halpem(6) used hypoxia and formula feeding beginning on P3 to induce NEC-like pathology. More recently, several laboratories have used hypoxia and formula feeding along with human NEC-associated microbial dysbiosis on P7–8 to induce NEC-like injury(7). MohanKumar induced NEC-like disease in P10 mice following TNBS exposure(8), and the McElroy laboratory has induced NEC-like injury in P14–16 mice by disrupting Paneth cells followed by enteral gavage of bacteria(9). While all these models produce phenotypes that are similar to the intestinal injury seen in human preterm infants with NEC, the wide variety of ages at which the models are performed is a potential confounding factor. This is important as the murine small intestine undergoes significant developmental changes from birth through 21–28 days of life(10). Furthermore, while mice are commonly used to model NEC, data comparing mouse intestinal developmental stages to equivalent developmental stages in the preterm human are lacking. Previous studies have attempted to compare development of murine and humans via comparison of microscopy, microbiomes, immunological components, and some specific small intestine enzymes (11–13). However, to date, no study has investigated a direct comprehensive comparison of murine and human small intestinal epithelium with the goal of defining equivalent developmental stages in mice and the preterm human. This is critical as NEC incidence is developmentally regulated, occurring primarily between 28 and 34 weeks of corrected gestational age(14) in humans. Our objective was to compare markers of intestinal epithelial development in both mice and humans, to better understand the gestational age in a mouse that corresponds to NEC susceptibility in humans. Our hypothesis is that a greater portion of intestinal development occurs during the post-natal period in mice compared to humans, with P14 mice most similar to preterm infants of 24 weeks gestation.

Author Manuscript Author Manuscript Author Manuscript Author Manuscript

Methods

Mice

All animal experiments were performed according to protocols approved by The University of Iowa IACUC. C57BL/6J mice whose founders were purchased from Jackson Laboratories, were housed under standard conditions in an AAALAC-approved vivarium. Small intestines were harvested from C57B1/6J mice at postnatal days (P)l, 5, 7, 10, 14, 17, 21, 24, and 28 (n=8 per group).

Murine small intestine tissue samples were paraffin-embedded and sectioned at 5 μm then stained with anti-chromogranin A (enteroendocrine cells), or Alcian blue/Periodic Acid Schiff (goblet and Paneth cells)(15). Intestinal epithelial cells were manually quantified at 20X magnification per 100 epithelial cells, with greater than or equal to 1000 epithelial cells counted per mouse intestine, except for Paneth cells which were manually quantified at 40X as Paneth cells per crypt, with greater than or equal to 300 crypts counted per mouse intestine.

Gene expression (Table 1) was quantified as previously described(9, 16) and primers are listed in Table 2. Fold change in gene expression was determined by normalizing gene expression to β-actin (stable in mouse intestinal tissues from P1–P28).

Human

Premature human intestine was obtained from the Health Sciences Tissue Bank with approval from the University of Pittsburgh Institutional Review Board (IRB, Protocol number PR014100537) and in accordance with their anatomical tissue procurement guidelines. Deidentified term control samples were obtained from infants undergoing post necrotizing enterocolitis re-anastomosis (n of 4–7 for all ages) with a waiver of consent and approval of University of Pittsburgh IRB (PRO 14070508).

Human samples were paraffin embedded, sectioned at 5 μm and stained for the following: goblet cells with muc2 (H-300, Santa Cruz), Paneth cells with lysozyme C (C-19, Santa Cruz), and enteroendocrine cells with Chromogranin A (Abeam) as previously described(17). Confocal microscopy images were obtained (Leica SP8 microscope) and assembled in Volocity software (Perkin Elmer). Images were analyzed by a blinded team member to quantify the number of enteroendocrine, and goblet cells per villus and Paneth cells per crypt.

Quantification of mRNA levels of specific genes (Table 1) was performed with quantitative real-time PCR using the Bio-Rad CFX96 Real-Time System(17). Samples were analyzed similarly as above, with equivalent human primers (Table 2). Fold change in gene expression was determined by normalizing to the housekeeping gene *RPLO* (stable in human tissue samples across ages sampled).

Author Manuscript Author Manuscript Author Manuscript Author Manuscript

Statistical analysis

Statistical analysis was performed using ΔΔ-CT as described(9). Statistical significance ($p<0.05$) was determined via ANOVA and appropriate tests of multiple comparisons using GraphPad Prism 8.

To directly compare relative development of the small intestine between murine and human samples, each age was assigned a relative time point. In mice, P1 was assigned to relative time point 1, P5 to relative time point 2, continuing through P28 which was assigned to relative time point 9. In humans, 17 weeks completed gestation was assigned to relative time point 1,18 weeks completed gestation was assigned to relative time point 2, continuing through term which was assigned to relative time point 8. To compare, each species at each time point was assigned a relative percentage of the maximum fold change detected. Comparison of the two trends was determined with linear regression changes over time.

To determine age-specific comparison trends, a dissimilarity matrix was created using XLSTAT 2017 (Addinsoft, Paris, France) to further compare clustering based on gene expression patterns with increasing age between neonatal mice and humans. To determine each age point in the matrix, the relative percentage of the maximum fold change for each individual sample for all genes examined at that age were averaged into a single number. Principle coordinate analysis (PCoA) was performed based on the dissimilarity matrix produced. Additionally, the relative percentage of the maximum fold change determined from above was plotted to their actual developmental time points (days in murine samples and weeks in human samples). An XY analysis was performed in GraphPad Prism to smooth the developmental curves. Murine and human plots were overlapped to describe the developmental stage similarities between the two species. Hashed lines were drawn to visually connect time points between mouse and human developmental stages.

Results

Comparison of genes involved in homeostasis:

The intestinal epithelium is in a constant state of turnover, and the immature small intestine experiences vast increases in surface area growth during development. Thus, we examined genes involved in regulation of proliferation (human *MKI67* and murine *Mki67* which code for Antigen Ki-67), apoptosis (human *BAX* and *BCL2*, and murine *Bax* and *Bell)*, and intestinal stem cell homeostasis (human *LGR5* and *BMI1*, and murine *Lgr5* and *Bmi1* which code for Leucine-rich repeat-containing G-protein coupled receptor 5 and Polycomb complex protein BMI-1, respectively) (Figure 1). Murine expression of *Mki67* significantly decreases from birth through P28, while no significant changes were seen in *MKI67* during human development. However, when comparing the relative trends over time, there were no significant differences between the two species. Murine and human ratios of the expression of *BAX* and *BCL2* stayed constant during intestinal development and showed no differences when comparing the trends over time. Murine expression of *Lgr5* significantly increased from birth to P10 and significantly decreased back to embryologie levels by P28. In contrast, human *LGR5* levels showed a trend towards decrease over time that became significant at term. When comparing murine and human expression trends over time, there were no

Author Manuscript Author Manuscript Author Manuscript Author Manuscript

significant differences between species. Murine expression of *Bmi1* remained relatively stable through P14 before decreasing significantly. No significant differences were seen in *BMI1* during human development. When comparing the developmental trends, only *BMI1* showed significant differences between mice and humans (p=0.0029).

Comparison of ErbB genes:

Since the ErbB receptor tyrosine kinases play an integral role in epithelial biology of the small intestine, we next quantified mRNA levels for all four family members in murine and human tissues (Figure 2). Murine *Egfr* (also known as *ErbBl*) showed a steady and significant decrease in expression from P7 to P28. This was not seen in the human tissues, and when comparing the two species, there were significant differences in *EGFR* expression trends during development (p=0.0008). Murine *Erbb2* and *Erbb3* declined in expression through P24 before returning to embryonic values on P28; in contrast, human tissues showed no significant changes in either over time. When comparing the developmental trends of *ERBB2* and *ERBB3* expression, no significant differences were seen between the two species. Mouse *Erbb4* was largely undetectable until P17 when it became elevated to 100 times the embryonic level at P28. While this same dramatic increase was not seen with human *ERBB4*, mouse and human expression trends did not significantly differ.

Comparison of structural genes:

To examine the structural components of the intestinal epithelium, we quantified mRNA levels of the cellular adhesion molecule E-cadherin, and the tight junction components ZO-1 and Occludin (Figure 3). Murine *Cdh1* (codes for E-cadherin) increased modestly but significantly from birth to P10 and decreased through adulthood back to newborn levels, while human tissue expression of *CDH1* stayed constant during development. Murine *Tjp1* (codes for ZO-1) expression showed modest but significant decreases from birth through adulthood while human *TJP1* showed a non-significant trend of increasing expression. Murine *Ocln* (codes for Occludin) expression showed similar patterns of decrease from P5 through adulthood as *Tjp1*. Human *OCLN* expression reached a significant peak at 18 weeks of gestation and similarly decreased toward term gestation. When comparing the developmental trends, only *TJP1* showed significantly different patterns between mice and humans (p<0.0001).

Comparison of epithelial cell specific genes:

We next quantified expression of several epithelial cell type-specific genes (Figure 4). Murine *Chga* (codes for Chromagranin A, a specific marker of enteroendocrine cells) expression stayed constant through the first two weeks of life before becoming significantly decreased at P24 and P28, while human *CHGA* levels remained stable throughout development. Murine *Dclk1* (codes for serine/threonine-protein kinase DCKL1, a specific marker of tuft cells) expression was stable from birth to P28, except for significant decreases in expression at P17 and P21. Human *DCLK1* expression varied greatly in 17-and 18-week gestation tissues, but also exhibited stable expression during development. Murine *Gp2* (codes for Pancreatic secretory granule membrane major glycoprotein GP2, a specific marker of M cells) significantly increased over time reaching an average of 4 times the embryonic levels by P28; however, there was marked variability in expression levels

Author Manuscript Author Manuscript Author Manuscript Author Manuscript

between individual mice. Human *GP2* also had marked sample variability but remained stable throughout development. When comparing the developmental trends, only *GP2* showed significant differences between murine and human developmental patterns (p=0.0011). *Muc2* (codes for murine Mucin 2, specific to goblet cells) was stably expressed from birth to P14 and decreased until becoming significantly lower than embryonic values at P28. *MUC2* (codes for human Mucin 2) remained stable over time. *Tff3* (codes for murine Trefoil factor 3 in goblet cells) increased over time, becoming significantly higher than embryonic levels at P28. *TFF3* (codes for human Trefoil factor 3) also increased over time, although not significantly. Neither *MUC2* nor *TFF3* expression patterns were significantly different between mouse and human tissues. However, we noted that the relative developmental expression patterns for both *MUC2* and *TFF3* were strikingly similar in both species.

Paneth cells are unique among intestinal epithelial cells as they possess dense granules containing multiple antimicrobial peptides. Murine expression of *Reg3γ* (codes for regenerating islet-derived protein 3) is fairly minimal until P21, when it quickly increases reaching almost a 1000-fold increase by P28. Human *Reg3α* (the homologue of murine *Reg3γ*) is also minimal from 17 to 23 weeks of gestation, but by term, *Reg3α* levels are significantly increased to an average of 20,000 times that of the level at 17 weeks. When comparing the two species, both demonstrate almost no expression until the end of intestinal development where there is a significant and massive increase in the relative expressions. A similar pattern is seen with *Lyzl* (codes for murine lysozyme-1) and *Defal* (codes for murine alpha defensin-1) which are minimally expressed through P10 followed by a significant elevation from P14-P28. *LYZ* (codes for human lysozyme-1) and *DEFA5* (the human homologue to murine *Defal*) are stable at minimal levels from 17 weeks of gestation through 23 weeks of gestation, but by term express significant increases in mRNA levels. In comparing the relative trends in development between mouse and human tissues, genes for both lysozyme and defensins show similar patterns of minimal expression in early development followed by steep increases over time. No significant differences were seen between murine and human *REG3, LYZ*, or *DEFA* developmental patterns.

Comparisons of cell quantification:

Lastly, to determine if our mRNA quantification scheme reflected cellular content, manual cell counts of enteroendocrine, goblet and Paneth cells were performed in both murine and human samples by immunostaining (Figure 5). For both species, the quantity of enteroendocrine cell counts showed were stable over time. Goblet cell counts in both murine and human samples remained relatively stable over time. Murine Paneth cells were not seen prior to P10, when they began to significantly increase over time. Human Paneth cells were negligible from 17 to 23 weeks completed gestation, but by term gestation were significantly increased in number. When comparing the developmental trends, all cell types quantified showed similar developmental patterns over time.

Direct comparison of developmental timing between mouse and human samples:

The objective of this study was to compare markers of intestinal development in both mice and humans, to better understand the gestational age in a mouse that corresponds to NEC

Author Manuscript Author Manuscript Author Manuscript Author Manuscript

susceptibility in humans. To determine this, we next took the relative trends in development for each gene in each species that had similar relative developmental patterns and mapped them to their actual developmental age instead of relative time points. These genes were compared using Principle Coordinate Analysis to determine similarities (Figure 6A). Mouse genes from P1–P17 days clustered in similar proximity to human genes from 17–23 weeks of completed gestational age. To further define similarities, genes from secretory epithelial cells (goblet, enteroendocrine, and Paneth cells) were compared in a second Principle Coordinate Analysis (Figure 6B) which showed even tighter clustering of mouse genes from P1–P17 days to human genes from 17–23 weeks completed gestation. We grouped the genes into three general developmental patterns: increasing, stable, or decreasing over time. Corresponding genes from both species were overlaid on top of each other to match similar patterning (Figure 6C). In this fashion, similar trends in development could be matched and correlated to each species' actual ages. Based on this analysis, for example, P14 mouse intestine appears to model human intestine at 22–23 weeks completed gestation, while P28 murine intestine is most similar to human tissue at term.

Discussion

Development of the mammalian intestinal tract requires the complex interaction of a multitude of genes representing many different cell types. During maturation, the gut develops from a simple tube into a mature organ that represents the largest surface area of the body(18), the largest lymphoid organ in the body, and houses the majority of the human microbiome(19). Understanding intestinal development is becoming increasingly important as modem neonatology pushes the limits of viability earlier and earlier(20, 21) creating a subset of patients who have an increasingly under-developed fragile intestine. Due to the limited availability of human-derived tissues, animal models remain critical to further our understanding of human diseases of the intestine(4). To better understand the pathophysiology of NEC, investigators have made use of many different model organisms (e.g. rats, mice, rabbits, quails, piglets, and nonhuman primates) and conditions to simulate the pathophysiology seen in NEC(4, 5, 22, 23). Each animal has distinct advantages and drawbacks related to their preterm viability, body size, genetic variability, and cost. For example, the pig has several distinct advantages for translational research including their similar genome, metabolic processes, microbial composition, and fecal transit time(24). At the same time, piglets do not appear to possess Paneth cells, have different development and distribution of their Peyer's patches, have an accelerated growth rate, are extremely costly, have limited analytical tools, and develop NEC-like injury in the entire GI tract as opposed to the distal small intestine seen in humans and mice(4, 22, 24–28).

Mice remain the most commonly utilized animal model to study diseases of the human intestine due to their low cost, easy maintenance, and rapid reproduction rate. Previous studies over the years have attempted to compare murine and human small intestine. McCracken and Lorenz illustrated the critical interactions that must occur between the microbiome and the host during intestinal development(29), and Mestas evaluated critical immunological similarities and differences between mice and humans(13), while Nguyen compared murine and human gastrointestinal tracts microscopically and morphologically. Nguyen discovered that the digestive tract is strongly conserved in mice and humans

Author Manuscript Author Manuscript Author Manuscript Author Manuscript

including conservation of secretory cells such as goblet and Paneth cells, but yet these differ in their intestinal distribution(11), however, to our knowledge, a direct detailed comprehensive comparison of the developmental patterns between humans and mice is lacking, primarily due to a lack of access to human tissues. To address this gap in knowledge, we directly compared the expression of genes that control intestinal structure, homeostasis and development of the many various epithelial cell types during development in both mice and humans, as well as several individual cell types.

Our initial hypothesis was that murine intestinal development is significantly delayed compared to that of the human, with postnatal day P14 mice most resembling the intestine of preterm infants who have completed 24 weeks of gestation. Our results examining the developmental patterns of twenty genes and three epithelial cell types show that the human and mouse do indeed have marked similarity in their intestinal development, though not all genes show similar patterns. In general, our data show that pre-viable human fetal intestine is most similar to newborn C57BL/6J mice, human intestine around 22–24 weeks completed gestation is most similar to mouse intestine at P14–17, and human term intestine is most similar to mouse intestine at P28.

The intestinal tract of both mice and humans contains the largest bodily surface area that is exposed to an external environment 18), and yet is covered with an epithelial layer that in both species is just a single cell layer thick. In order to maintain protection for the host while allowing for nutrient absorption, this epithelial lining is continuously replenishing itself and consists of many specialized cell types working in concert. Proliferation by stem cells within the intestinal crypt supplies a constant stream of new cells to drive epithelial self-renewal, leading to the turnover of the epithelial layer every 4–5 days in humans(30). Both mouse and human tissues show similar trends of proliferation and apoptosis over time suggesting similar growth patterns. However, we noted different patterns in intestinal stem cell marker expression. Crypt-base columnar cells express the specific marker *LGR5* and are located in the crypt base between Paneth cells where they actively proliferate(31). A second population (located above the crypt base) express *BMI1* and have been hypothesized to be quiescent “reserve” stem cells until an injury occurs, at which time they begin to actively proliferate(32). Our data show that both mice and humans experience a steady significant drop off of *LGR5* expression during development. This differs from the expression of *BMI1* which mirrors *Lgr5* in mice, but shows no decline in humans. This may be due to our tissue sample bias as all our human term samples had previously been injured so are expected to have some level of intestinal adaptation.

An important regulator of epithelial homeostasis is the ErbB family of tyrosine kinase receptors(33). The ErbB family includes the prototypic member EGFR/ErbBl as well as ErbB2, ErbB3, and ErbB4. After binding to their ligands, ErbBs signal as dimers through increased kinase activity and provide docking sites for downstream substrates and adapter proteins. We found some intriguing trends in ErbB family member expression over time in comparing human and mouse tissues. Patterns and timing of *ERBB2* and *ERBB3*e xpression were similar in both species, while *EGFR* and *ERBB4* diverged. In mice, *ErbBl* showed a steady and significant decrease in expression over time while human *EGFR* levels increased from 17–23 weeks of completed gestation before beginning a trend towards decreased

Author Manuscript Author Manuscript Author Manuscript Author Manuscript

expression. Unfortunately, our sample set lacks infants from 24–36 weeks of gestation which would help us understand if murine and human tissues have different patterns of *EGFR* expression, or if the downward trend seen in mice happens after 23 weeks in humans. *ERBB4* expression was also different between the two species. In mice, the expression pattern of *ErbB4* is minimal from birth through P17, at which time they experience a dramatic increase in expression that persists through P28. Human *ERBB4* shows an increase from 17–23 weeks gestation followed by a return to embryonic levels by term. As the ErbB family has been shown to be able to impact intestinal diseases such as NEC (15, 34), further exploration is warranted.

Lastly, goblet cells are the major secretory cell located in the intestinal epithelium and are responsible for producing mucin, trefoil peptides, resistin-like molecules-β, and Fey binding protein(35). Our data show a marked similarity between gene expression of both *MUC2* and *TFF3* over time in both mice and humans. However, a close relative of the goblet cell is the antimicrobial secreting Paneth cell(36), which resides in the small intestinal crypts and secretes several antimicrobial substances including α-defensins (cryptdins in mice), β-defensins, Reg3, and lysozyme(37). Both murine and human tissues showed similar patterns of expression with massive increases occurring over time. Interestingly, genes specific to Paneth cell function in humans are delayed compared to other epithelial genes. While most murine gene expression at P14–17 show similarity to human intestinal genes at 22–23 weeks gestation, changes in murine Paneth cell genes seen at P14–17 are not seen in humans until after 24 weeks. As Paneth cells are a critical component to intestinal homeostasis and immunity(38), this represents an important factor when comparing murine and human tissues for the study of human diseases, especially as intestinal diseases of prematurity such as spontaneous intestinal perforations and NEC appear to be developmentally regulated(2, 14).

It is important to note that our study has several limitations. The first is the overall limited availability of human samples. Procurement of human preterm intestinal samples has been a recurrent problem in NEC research(39). Our human samples were obtained from elective terminations from pregnancies at periviable gestational ages. Since these samples came from deceased fetuses, our samples may not be reflective of what is truly occurring in a healthy living infant. Our samples were also limited by a lack of access to human samples from 24 weeks to term gestation in our biorepository. The incidence of non-inflammatory/necrotic intestinal pathology (such as ileal atresia) that requires surgical intervention in premature infants is very low. As our murine samples were all from healthy mice, we did not want to further complicate comparisons by introducing human pathology. A second limitation is that clinical information for our human samples was not available given the nature of the IRB approval. This data also includes the corrected gestation of our term samples. The standard of care at the University of Pittsburgh is for infants to undergo post-NEC re-anastomosis surgeries when the infant is near term gestation, so it is reasonable to assume that our term cohort of samples represent term tissue. Furthermore, our term samples were from infants who had previously developed NEC and so we cannot be sure that intestinal adaptation didn’t affect our results. Intestinal adaptation is a natural compensatory process that occurs following intestinal resection, where the intestine undergoes both structural and functional changes to enhance nutrient and fluid absorption in the remaining bowel(40). However, as

Author Manuscript Author Manuscript Author Manuscript Author Manuscript

term healthy infants rarely have small intestinal biopsies/tissue samples obtained, we believe that this is as close as we can get to an accurate representation of term human small intestinal tissues. Further, the vast majority of the genes and cell types we profiled showed congruence with mouse tissues suggesting that our term tissues are indeed a valid representation of normal human intestinal development.

In summary, our study quantified important epithelial genes and cell types during development in both the mouse and human, and further, compared the two species for developmental congruence. Animal models, including mouse models, are critical in aiding our understanding of diseases of the immature intestine, including NEC, which despite carrying significant morbidity and mortality, is poorly understood as the exact pathogenesis remains unknown. However, utilizing animals modeling disease processes that occur during organ development requires careful matching of developmental stages. Our data directly compares murine and human stages during development. This data allows a better understanding of the overall development of the small intestine and will importantly provide guidance to relate findings from mouse models to human diseases such as NEC.

Financial support for this project was provided by:

SJM is supported by the National Institutes of Health DK097335 and the Stead Family Department of Pediatrics, Carver College of Medicine at the University of Iowa. MG is supported by K08DK101608, R03DK111473 and R01DK118568 from the National Institutes of Health, March of Dimes Foundation Grant No. 5xFY17–79, the Children's Discovery Institute of Washington University and St. Louis Children's Hospital, and the Department of Pediatrics at Washington University School of Medicine, St. Louis. MRF is supported by R01DK095004 and a Senior Research Award from the Crohn's and Colitis Foundation.

References:

1. Howson CP, Kinney MV, McDougall L, Lawn JE, Born Too Soon Preterm Birth Action G 2013 Born too soon: preterm birth matters. Reprod Health 10 Suppl 1:S1. [PubMed: 24625113]
2. Patel RM, Kandefer S, Walsh MC, et al. 2015 Causes and timing of death in extremely premature infants from 2000 through 2011. N Engl J Med 372:331–340. [PubMed: 25607427]
3. Walsh MC, Bell EF, Kandefer S, et al. 2017 Neonatal outcomes of moderately preterm infants compared to extremely preterm infants. Pediatr Res 82:297–304. [PubMed: 28419085]
4. Ares GJ, McElroy SJ, Hunter CJ 2018 The science and necessity of using animal models in the study of necrotizing enterocolitis. Semin Pediatr Surg 27:29–33. [PubMed: 29275813]
5. Jilling T, Simon D, Lu J, et al. 2006 The roles of bacteria and TLR4 in rat and murine models of necrotizing enterocolitis. J Immunol 177:3273–3282. [PubMed: 16920968]
6. Halpern MD, Khailova L, Molla-Hosseini D, et al. 2008 Decreased development of necrotizing enterocolitis in IL-18-deficient mice. Am J Physiol Gastrointest Liver Physiol 294:G20–26. [PubMed: 17947451]
7. Good M, Sodhi CP, Yamaguchi Y, et al. 2016 The human milk oligosaccharide 2'-fucosyllactose attenuates the severity of experimental necrotising enterocolitis by enhancing mesenteric perfusion in the neonatal intestine. Br J Nutr 116:1175–1187. [PubMed: 27609061]
8. MohanKumar K, Kaza N, Jagadeeswaran R, et al. 2012 Gut mucosal injury in neonates is marked by macrophage infiltration in contrast to pleomorphic infiltrates in adult: evidence from an animal model. Am J Physiol Gastrointest Liver Physiol 303:G93–102. [PubMed: 22538401]
9. White JR, Gong H, Pope B, Schlievert P, McElroy SJ 2017 Paneth-cell-disruption-induced necrotizing enterocolitis in mice requires live bacteria and occurs independently of TLR4 signaling. Dis Model Mech 10:727–736. [PubMed: 28450472]
10. McElroy SJ, Weitkamp JH 2011 Innate Immunity in the Small Intestine of the Preterm Infant. NeoReviews 12:e517–e526. [PubMed: 22639551]

Author Manuscript Author Manuscript Author Manuscript Author Manuscript

11. Nguyen TL, Vieira-Silva S, Liston A, Raes J 2015 How informative is the mouse for human gut microbiota research? Dis Model Mech 8:1–16. [PubMed: 25561744]
12. Hugenholtz F, de Vos WM 2018 Mouse models for human intestinal microbiota research: a critical evaluation. Cell Mol Life Sei 75:149–160.
13. Mestas J, Hughes CC 2004 Of mice and not men: differences between mouse and human immunology. J Immunol 172:2731–2738. [PubMed: 14978070]
14. Yee WH, Soraisham AS, Shah VS, Aziz K, Yoon W, Lee SK 2012 Incidence and timing of presentation of necrotizing enterocolitis in preterm infants. Pediatrics 129:e298–304. [PubMed: 22271701]
15. McElroy SJ, Castle SL, Bernard JK, et al. 2014 The ErbB4 ligand neuregulin-4 protects against experimental necrotizing enterocolitis. Am J Pathol 184:2768–2778. [PubMed: 25216938]
16. Fricke EM, Elgin TG, Gong H, et al. 2018 Lipopolysaccharide-induced maternal inflammation induces direct placental injury without alteration in placental blood flow and induces a secondary fetal intestinal injury that persists into adulthood. Am J Reprod Immunol 79:e12816. [PubMed: 29369434]
17. Good M, Sodhi CP, Egan CE, et al. 2015 Breast milk protects against the development of necrotizing enterocolitis through inhibition of Toll-like receptor 4 in the intestinal epithelium via activation of the epidermal growth factor receptor. Mucosal Immunol 8:1166–1179. [PubMed: 25899687]
18. Helander HF, Fandriks L 2014 Surface area of the digestive tract - revisited. Scand J Gastroenterol 49:681–689. [PubMed: 24694282]
19. Gilbert JA, Blaser MJ, Caporaso JG, Jansson JK, Lynch SV, Knight R 2018 Current understanding of the human microbiome. Nat Med 24:392–400. [PubMed: 29634682]
20. Patel RM, Rysavy MA, Bell EF, Tyson JE 2017 Survival of Infants Bom at Periviable Gestational Ages. Clin Perinatol 44:287–303. [PubMed: 28477661]
21. Younge N, Goldstein RF, Bann CM, et al. 2017 Survival and Neurodevelopmental Outcomes among Periviable Infants. N Engl J Med 376:617–628. [PubMed: 28199816]
22. Sangild PT, Siggers RH, Schmidt M, et al. 2006 Diet- and colonization-dependent intestinal dysfunction predisposes to necrotizing enterocolitis in preterm pigs. Gastroenterology 130:1776–1792. [PubMed: 16697741]
23. Waligora-Dupriet AJ, Dugay A, Auzeil N, Huerre M, Butel MJ 2005 Evidence for clostridial implication in necrotizing enterocolitis through bacterial fermentation in a gnotobiotic quail model. Pediatr Res 58:629–635. [PubMed: 16189185]
24. Gonzalez LM, Moeser AJ, Blikslager AT 2015 Porcine models of digestive disease: the future of large animal translational research. Transi Res 166:12–27.
25. Myer MS 1982 Paneth cells in the pig-a controversial issue. J S Afr Vet Assoc 53:69. [PubMed: 7097712]
26. Puiman PJ, Stoll B, van Goudoever JB, Burrin DG 2011 Enteral arginine does not increase superior mesenteric arterial blood flow but induces mucosal growth in neonatal pigs. J Nutr 141:63–70. [PubMed: 21106927]
27. Ziegler A, Gonzalez L, Blikslager A 2016 Large Animal Models: The Key to Translational Discovery in Digestive Disease Research. Cellular and molecular gastroenterology and hepatology 2:716–724. [PubMed: 28090566]
28. Litten-Brown JC, Corson AM, Clarke L 2010 Porcine models for the metabolic syndrome, digestive and bone disorders: a general overview. Animal 4:899–920. [PubMed: 22444262]
29. McCracken VJ, Lorenz RG 2001 The gastrointestinal ecosystem: a precarious alliance among epithelium, immunity and microbiota. Cell Microbiol 3:1–11. [PubMed: 11207615]
30. van der Flier LG, Clevers H 2009 Stem cells, self-renewal, and differentiation in the intestinal epithelium. Annu Rev Physiol 71:241–260. [PubMed: 18808327]
31. Cheng H, Leblond CP 1974 Origin, differentiation and renewal of the four main epithelial cell types in the mouse small intestine. V. Unitarian Theory of the origin of the four epithelial cell types. Am J Anat 141:537–561. [PubMed: 4440635]
32. Yan KS, Chia LA, Li X, et al. 2012 The intestinal stem cell markers Bmil and Lgr5 identify two functionally distinct populations. Proc Natl Acad Sci U S A 109:466–471. [PubMed: 22190486]

Author Manuscript Author Manuscript Author Manuscript Author Manuscript

33. Frey MR, Brent Polk D 2014 ErbB receptors and their growth factor ligands in pediatric intestinal inflammation. Pediatr Res 75:127–132. [PubMed: 24402051]
34. Almohazey D, Lo YH, Vossler CV, et al. 2017 The ErbB3 receptor tyrosine kinase negatively regulates Paneth cells by PI3K-dependent suppression of Atohl. Cell Death Differ 24:855–865. [PubMed: 28304405]
35. Kandasamy J, Huda S, Ambalavanan N, Jilling T 2014 Inflammatory signals that regulate intestinal epithelial renewal, differentiation, migration and cell death: Implications for necrotizing enterocolitis. Pathophysiology 21:67–80. [PubMed: 24533974]
36. Clevers HC, Bevins CL 2013 Paneth cells: maestros of the small intestinal crypts. Annu Rev Physiol 75:289–311. [PubMed: 23398152]
37. Berman L, Moss RL 2011 Necrotizing enterocolitis: an update. Semin Fetal Neonatal Med 16:145–150. [PubMed: 21514258]
38. Bevins CL, Salzman NH 2011 Paneth cells, antimicrobial peptides and maintenance of intestinal homeostasis. Nat Rev Microbiol 9:356–368. [PubMed: 21423246]
39. Ralls MW, Gadepalli SK, Sylvester KG, Good M 2018 Development of the necrotizing enterocolitis society registry and biorepository. Semin Pediatr Surg 27:25–28. [PubMed: 29275812]
40. Dowling RH, Booth CC 1966 Functional compensation after small-bowel resection in man. Demonstration by direct measurement. Lancet 2:146–147. [PubMed: 4161381]

Author Manuscript Author Manuscript Author Manuscript Author Manuscript

Article Impact Questions:

1. **What is the key message of your article?**Intestinal epithelial developmental patterns are similar in mice and humans but vary according to the timing of normal birth.
2. **What does it add to the existing literature?**This is the first comprehensive direct comparison of intestinal epithelial developmental gene patterns between the mouse and human
3. **What is the impact?**The impact of our work helps to better define age equivalency when using mouse models to study diseases that impact the preterm human intestinal tract such as SIP or NEC.

Author Manuscript
Author Manuscript
Author Manuscript
Author Manuscript

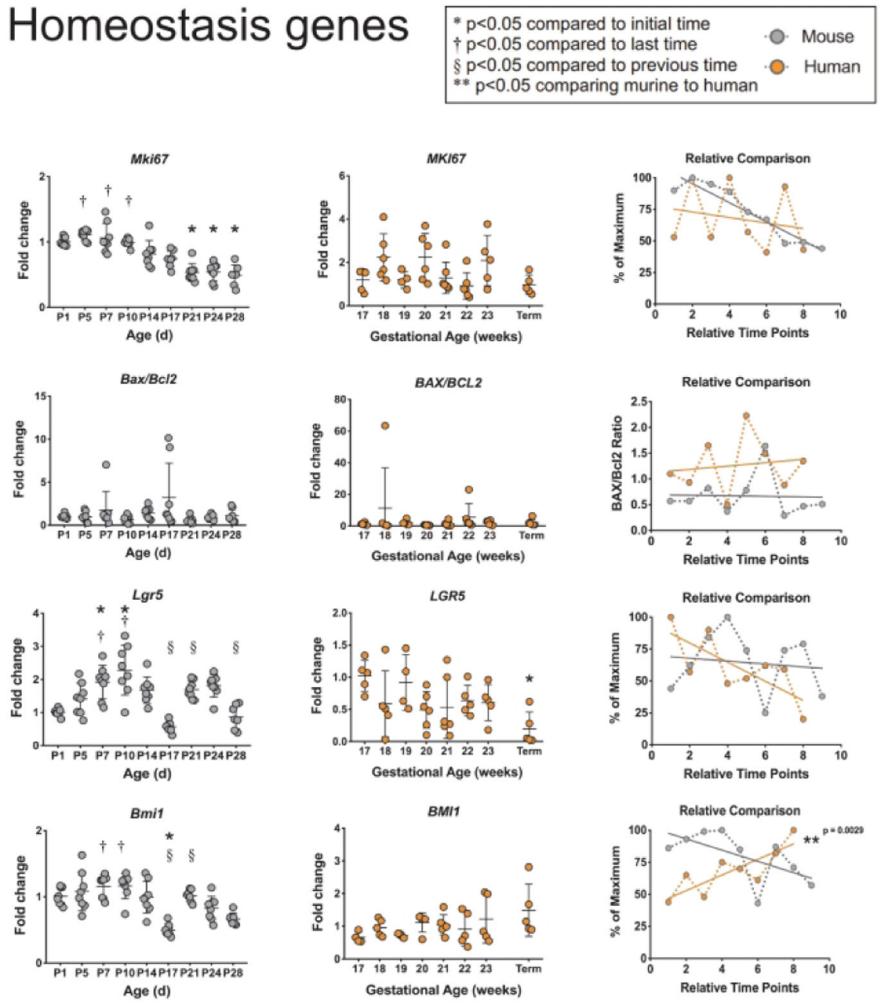

Figure 1: Comparison of homeostasis genes between murine and humans.

Homeostasis genes*MKI67, BAX/BCL2, LGR5*, and *BMI1*were evaluated in murine and human small intestines. Murine samples (far-left column in grey) show fold change with β-*actin*as a reference gene at ages shown (n=8 per group). Human samples (middle column in orange) show fold change with *RPLO* as a reference gene at ages shown (n=4–7). Significant differences are denoted as shown. Relative comparison (far-right column) of murine (grey) to human (orange) developmental trends as percent of maximum over time points. Linear regression was calculated to determine statistical significance between time points.

Author Manuscript Author Manuscript Author Manuscript Author Manuscript

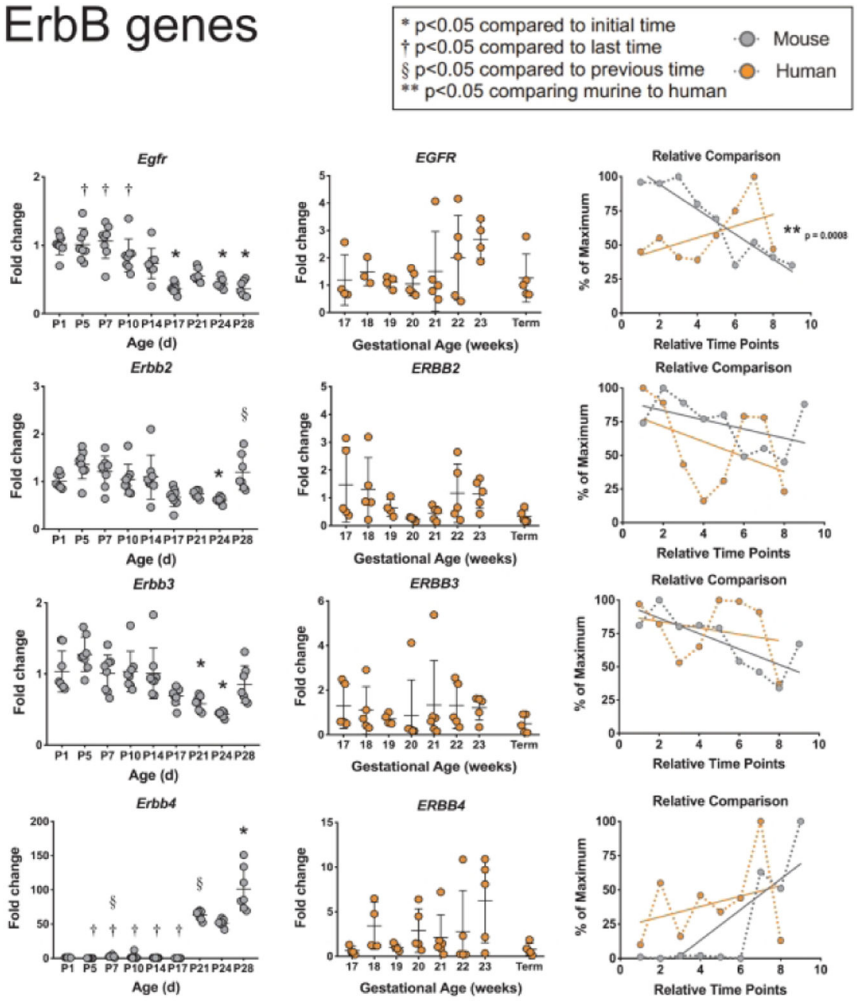

Figure 2: Comparison of ErbB genes between murine and humans.

ErbB genes *EGFR and ERBB2–4* were evaluated in murine and human small intestines as described in Figure 1.

Author Manuscript Author Manuscript Author Manuscript Author Manuscript

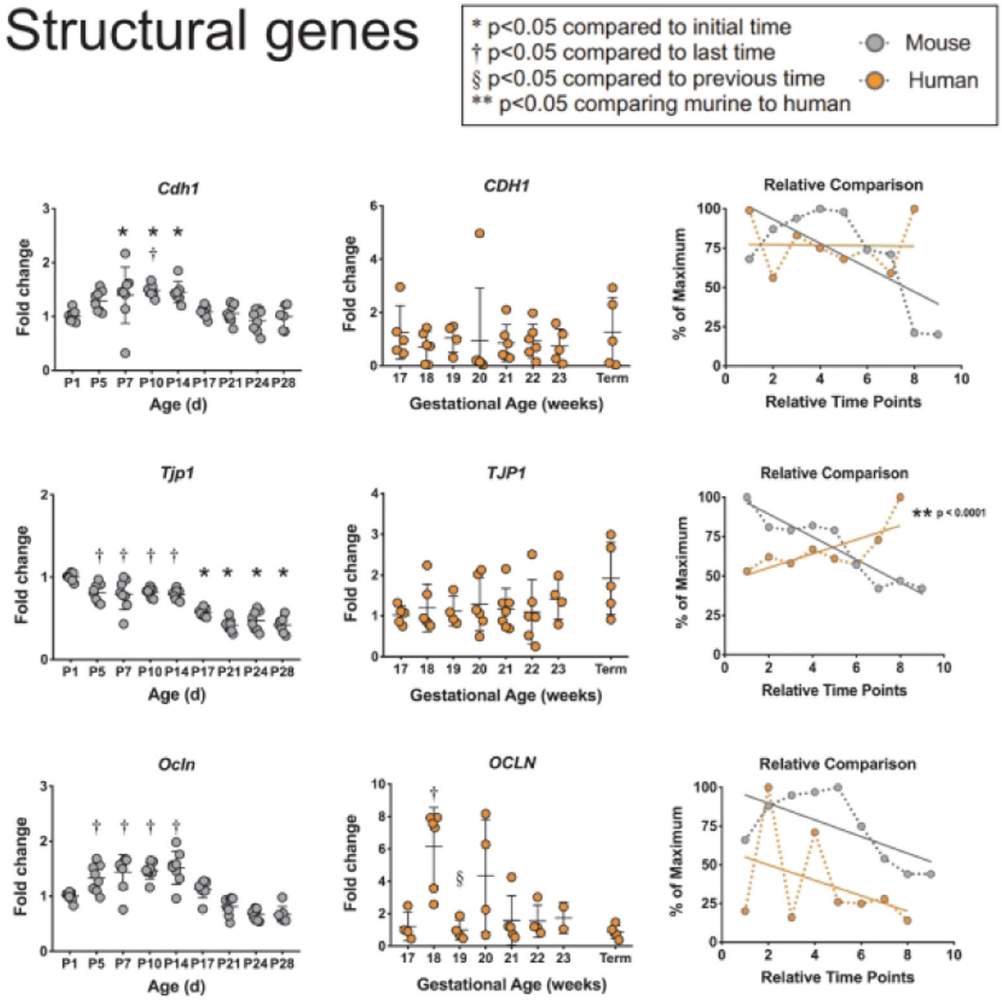

Figure 3: Comparison of structural genes between murine and humans.

Structural genes *CDH1, TJP1*, and *OCLN* were evaluated in murine and human small intestines as described in Figure 1.

Author Manuscript Author Manuscript Author Manuscript Author Manuscript

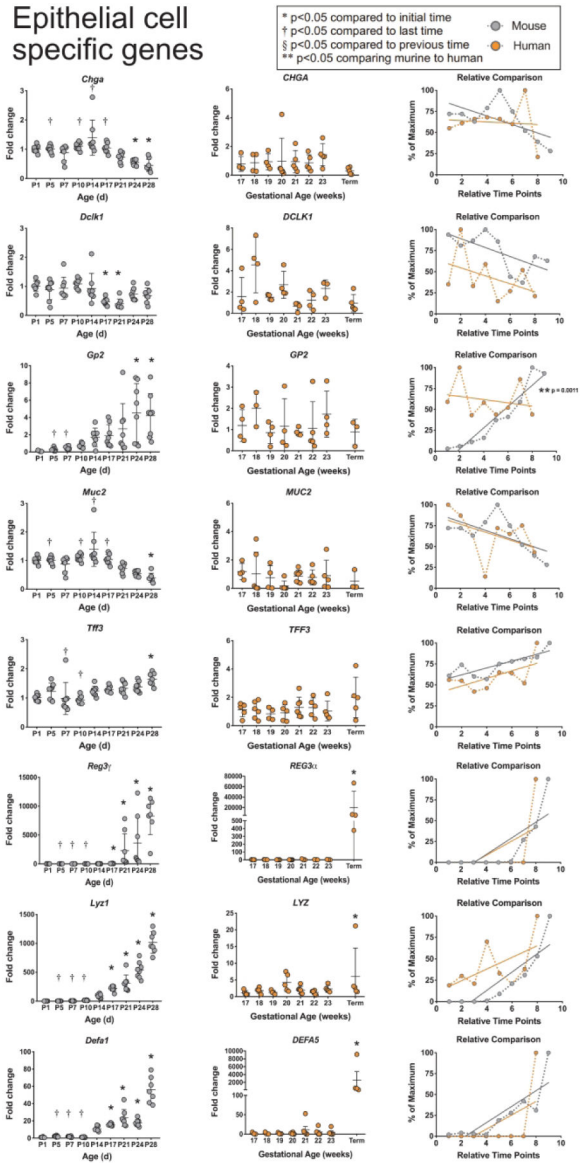

Figure 4: Comparison of epithelial cell specific genes between murine and humans.

Epithelial cell specific genes *CHGA, DCLK1, GP2, MUC2, TFF3, REG3γ/Reg3a, LYZ/Lyz 1*, and *DEFA5/Defa1* were evaluated in murine and human small intestines as described in Figure

Author Manuscript Author Manuscript Author Manuscript Author Manuscript

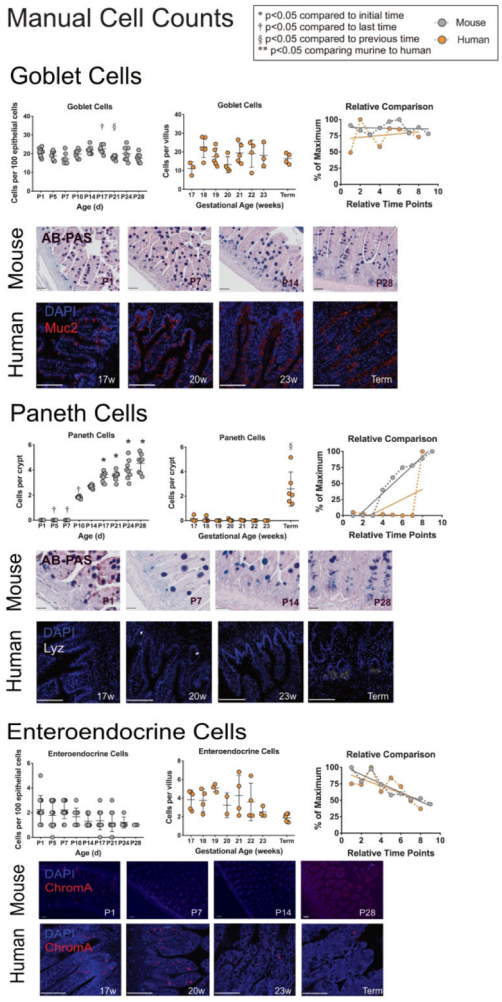

Figure 5: Quantification and comparison of enteroendocrine, goblet, and Paneth cells between murine and humans.

Manual cell counts of enteroendocrine, goblet and Paneth cells were quantified in mouse and humans. Murine samples were stained with Alcian-blue Periodic Acid Schiff (goblet cells and Paneth cells) or with α-Chromogranin A (enteroendocrine cells). Human samples were stained with a-Muc 2 (goblet cells), a-lysozyme (Paneth cells), or with α-Chromogranin A (enteroendocrine cells). Scale bars denote 50μm.

Murine samples (far-left column in grey) show positive cells per 100 epithelial cells for enteroendocrine, and goblet cells, and positive cells per crypt for Paneth cells. Counts were performed at ages shown (n=8 per group). Human samples (middle column in orange) show cells per villus for enteroendocrine and goblet cells, and cells per crypt for Paneth cells. Counts were performed at ages shown (n=4–7). Linear regression was calculated to determine statistical significance between time points.

Author Manuscript Author Manuscript Author Manuscript Author Manuscript

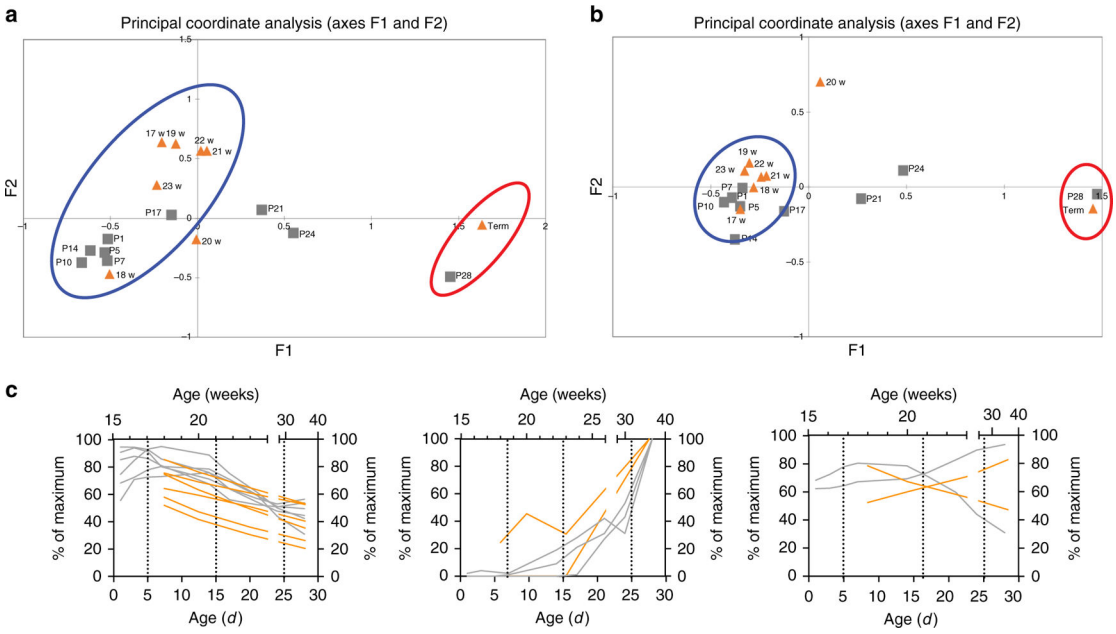

Figure 6: Direct age-based comparison of murine and human genes.

To determine age-based comparisons, a Principle Coordinate Analysis was generated using the maximum relative values from *REG3γ/Reg3a, LYZ/Lyz 1, DEFA5/Defa, MUC2, TFF3, CDH1, OCLN1, MK167, CHGA, DCLK1*, and *LGR5* (A), and a second Principle Coordinate Analysis was generated using the maximum relative values from *REG3γ/Reg3a, LYZ/Lyz 1, DEFA5/Defβ, MUC2, TFF3*, and *CHGA* (B) to determine relative similarities between developmental stages. In both analyses, murine genes from age P1–P17 were similar to human samples from age 17–23 weeks. To further delineate equivalent ages, the relative percentage of the maximum fold change was plotted to their developmental time points (days in murine samples and weeks in human samples) from *CDH1, OCLN1, MKI67, CHGA, DCLK1*, and *LGR5* (left plot), *REG3γ/Reg3a, LYZ/Lyz 1*, and *DEFA5/Defa* (center plot), and *MUC2*, and *TFF3* (right plot). An XY analysis was performed in GraphPad Prism to smooth the developmental curves. Murine (gray lines associated with the bottom X-axis and left Y-axis) and human plots (orange lines associated with the top X-axis and right Y-axis) were overlapped to describe the developmental stage similarities between the two species. Hashed lines were drawn to visually connect time points between mouse and human developmental stages.

Author Manuscript Author Manuscript Author Manuscript Author Manuscript

Table 1:

Epithelia cell proteins and their associated genes in mouse and human small intestine

Protein	Murine Gene	Human Gene
Structural		
E-cadherin	*Cdh1*	*CDH1*
Zonula occludens-1	*Tjp1*	*TJP1*
Occludin	*Ocln*	*OCLN*
Homeostasis		
Antigen KI-67	*Mki67*	*MKI67*
Apoptosis regulator BAX	*Bax*	*BAX*
Bcl2	*Bcl2*	*BCL2*
Leucine-rich repeat-containing G-protein coupled receptor 5	*Lgr5*	*LGR5*
Polycomb complex protein BMI-1	*Bmi1*	*BMI1*
ErbB		
Epidermal growth factor receptor	*Egfr*	*EGFR*
Receptor tyrosine-protein kinase erbB-2	*Erbb2*	*ERBB2*
Receptor tyrosine-protein kinase erbB-3	*Erbb3*	*ERBB3*
Receptor tyrosine-protein kinase erbB-4	*Erbb4*	*ERBB4*
Epithelial Cell Specific		
Chromagranin A	*Chga*	*CHGA*
Serine/threonine-protein kinase DCLK1	*Dclk1*	*DCLK1*
Pancreatic secretory granule membrane major glycoprotein GP2	*Gp2*	*GP2*
Goblet and Paneth Cells		
Mucin 2	*Muc2*	*MUC2*
Trefoil factor 3	*Tff3*	*TFF3*
Regenerating islet-derived protein 3	*Reg3γ*	*REG3α*
Lysozyme1	*Lyz1*	*LYZ*
Alpha Defensin	*Defa1*	*DEFA5*

Author Manuscript Author Manuscript Author Manuscript Author Manuscript

Table 2:

Listing of individual qPCR primers used for each murine and human gene

Gene	Murine	Human Forward Primer	Human Reverse Primer
Structural			
CDH1	Mm01247357_m1, Taqman Life Technologies	ACACAGGAGTCATCAGTGTGGTCA	AGCTGTTGCTGTTGTGCTTAACCC
TJP1	Mm00493699_m1, Taqman Life Technologies	GCCATTCCCGAAGGAGTTGA	ATCACAGTGTGGTAAGCGCA
OCLN	Mm00500912_m1, Taqman Life Technologies	GCCTCTCTCCATCAGACACC	TAAACCAATCTGCTGCGTCCTA
Homeostasis			
MKI67	Mm01278617_m1, Taqman Life Technologies	GACCTCAAACTGGCTCCTAATC	GCTGCCAGATAGAGTCAGAAAG
BAX	Mm00432051_m1, Taqman Life Technologies	TCATGGGCTGGACATTGGAC	GAGACAGGGACATCAGTCGC
BCL2	Mm00477631_m1, Taqman Life Technologies	AACATCGCCCTGTGGATGAC	GACTTCACTTGTGGCCCAGAT
LGR5	Mm00438890_m1, Taqman Life Technologies	TCTTGCGGGAAACGCTCTGACATA	TTAGCATCCAGACGCAGGGATTGA
BMI1	Mm03053308_g1, Taqman Life Technologies	GCTGGTTGCCCATTGACAG	AAATCCCGGAAAGAGCAGCC
ErbB			
EGFR	Mm00433023_m1, Taqman Life Technologies	TATTGATCGGGAGAGCCGGA	TCGTGCCTTGGCAAACTTTC
ERBB2	Mm00658541_m1, Taqman Life Technologies	GCACCATGGAGCTGGCG	CTGTGCCGGTGCACACTTG
ERBB3	Mm01159999_m1, Taqman Life Technologies	TGACTGGAGGGACATCGTGA	TTGGTCAATGTCTGGCAGTCT
ERBB4	Mm01256793_m1, Taqman Life Technologies	GTTCAGGATGTGGACGTTGC	CTGCCGTCACATTGTTCTGC
Epithelial Cell Specific			
CHGA	Mm00514341_m1, Taqman Life Technologies	AGGAAGAAGGCCCCACTGTA	GTGCTCCTGTTCTCCCTTCC
DCLK1	Mm00444950_m1, Taqman Life Technologies	GCATTTCAATGAGGACGGGC	GAAGTGCTCCAGCTCCATGT
GP2	Mm00482557_m1, Taqman Life Technologies	ATGGCATCACCAACCACACT	TGGATGGGTCTCGTGGAAC

Pediatr Res. Author manuscript; available in PMC 2019 December 27.

Author Manuscript Author Manuscript Author Manuscript Author Manuscript

Gene	Murine	Human Forward Primer	Human Reverse Primer
Goblet and Paneth Cells			
MUC2	Mm01276696_m1, Taqman Life Technologies	AGGTGCTGATCAAGACCGTGCATA	ATGTCCACCACGTAGTTGATGCCA
TFF3	Mm00495590_m1, Taqman Life Technologies	CTCCTGGACCATGAAGCGAG	TGAAACACCAAGGCACTCCA
Reg3γ / REG3a	Mm00441127_m1, Taqman Life Technologies	TATCTGTGTGTCCTCCCGCT	AGGAAAGCAGCATCCAGGAC
Lyz1 / LYZ	Mm00657323_m1, Taqman Life Technologies	CCTGCAGTGCTTTGCTGCAAGATA	TCTCCATGCCACCCATGCTCTAAT
Defa1 / DEFA5	Mm02524428_m1, Taqman Life Technologies	CTCCAAAGCATCCAGGCTCA	CAAGCTCAGCAGCAGAATGC